CADiff: a software and method to numerically model diffusion and reactive–diffusion in multi-component systems

Marek DANIELEWSKI[a], Bartlomiej WIERZBA[b]

Interdisciplinary Centre for Materials Modeling, Faculty of Materials Science and Ceramics
AGH University of Science and Technology, Al. Mickiewicza 30, 30-059 Cracow, Poland

[a]daniel@agh.edu.pl, [b]bwierzba@agh.edu.pl; Fax: +48 126172493

Abstract.

We present the software and method CADiff which allows for numerical simulation of interdiffusion and reactive diffusion processes. With two examples we demonstrate the effectiveness of our method. The known methods on the reactive and interdiffusion are significantly extended as follows: *i*) the diffusion fluxes are defined in the volume fixed reference frame that is rigorously defined *ii*) the Darken method is extended and allows analyzing the non ideal alloys showing different molar volumes, *iii*) the boundary conditions take into account both the interdiffusion and reactive diffusion and *iv*) the flux constraints are used to couple processes occurring at different time scales. We demonstrate solutions of the interdiffusion in Fe-Ni-Cu alloy and heterogeneous reaction between multicomponent alloy and oxidant. The interdiffusion can be computed starting from the Fick's constitutive diffusion flux formula to the combined Darken-Onsager approach. It allows modeling pure interdiffusion in multi-component systems as well as a wide class of the reaction-diffusion problems associated with solid state chemistry, corrosion, surface treatment etc.

Keywords: diffusion, interdiffusion, reaction diffusion, oxidation, chemical interdiffusion.

1. Introduction.

The quantitative models of the processes and material behavior can be very useful in testing material stability, estimating required properties and predicting their "life time". The reliable and simple simulation software considerably accelerates both the research and the development. It helps in designing and production of new materials.

The heterogeneous reactions in ternary system were analyzed by Wagner [1-4]. These are essentially the quasi-equilibrium processes (chemical diffusion, and reactions at interfaces) that take place under the influence of chemical potential gradient [5,6]. He was first to notice that the oxidized component enters the oxide phase as a result of the surface reaction and of the diffusion through alloy|oxide interface. The non-reacting elements diffuse into the interior of the alloy [3].

The both Onsager [7,8] and Darken [9] methods are commonly used in nonequilibrium thermodynamics to describe diffusion in solids. The key Darken postulate that the total mass flow is a sum of the diffusion and drift flows was applied for the description of the diffusion in multi-component solid solution [10,11]. The equations of mass conservation, the appropriate expressions describing the fluxes and the postulate of constant molar volume of the system allowed the quantitative description of the diffusion transport process in the open as well as closed system, i.e., in the diffusion couple of the finite thickness. The method describes interdiffusion when intrinsic diffusivities depend on composition and allows including activities of components [10].

In this software the Darken method is further extended to include the variable and/or different molar volumes, e.g., the Vegard law [12]. Moreover, we rigorously combine interdiffusion and reactive diffusion by broadening the Wagner boundary condition [3]. The method presented here and simulation package allows modeling the wide range of processes that can be treated as one-dimensional diffusion with convection (Darken drift) and reaction at interfaces. Classical examples shown are:

- Interdiffusion in the closed multi-component systems, e.g., diffusion mixing, evolution of gradient materials and multi-layer systems.
- Reaction-diffusion, i.e., the coupled interdiffusion and reactive diffusion due to the chemical reaction at the moving interface.

In what follows we consider the processes where the diffusivities may differ by orders of magnitude and number of components is unlimited. Consequently, the problem exhibits different time scales, e.g., the slow chemical diffusion (in the growing layer) and fast interdiffusion in multi-component mixture (alloy, intermetallic compound, etc.). The two-scale computational methods of modeling were used by many authors to model the mechanical properties of materials with microstructure and two-scale simulations were proven to be efficient and reliable [13,14]. In most cases system of equations were solved in different time scales. In this work we use the concept of the flux limiter [15]. The interdiffusion method, the reaction-diffusion and simulation results are shown in the following sections.

2. Interdiffusion in multicomponent open systems

Depending on the availability of the data and the required accuracy, CADiff allows selecting: *i*) the constitutive equations for diffusion flux, Fig. 1 and section 2.3, *ii*) the equation of state, section 2.2, *iii*) expression for diffusivities, section 2.4 and *iv*) the form of the known or computed reaction flux between alloy and surrounding.

1) **Laws**:

a) Conservation of mass (Section 2.1):

$$\frac{\partial c_i}{\partial t} + \mathrm{div} J_i = 0, \quad i = 1,\dots,r$$

b) Equation of state (Section 2.2)

c) Diffusion flux (Section 2.3)

d) Diffusivities (Section 2.4)

2) Boundary conditions and reaction flux (Sections 2.5)

Flux formulae can be chosen from the set of the following constitutive equations:

Diffusion and Convection:

Darken-Onsager (DO)

$$J_i = \sum_{j=1}^{r} L_{ij} X_j + c_i \upsilon^D, \qquad i = 1,\dots,r$$

or

Darken-Nernst-Planck (DNP)

$$J_i = B_i c_i X_i + c_i \upsilon^D, \qquad i = 1,\dots,r$$

or

Darken-Fick (DF)

$$J_i = -D_i \ \mathrm{grad}\ c_i + c_i \upsilon^D, \qquad i = 1,\dots,r$$

or

Diffusion only:

Onsager (O)

$$J_i = \sum_{j=1}^{r} L_{ij} X_j, \qquad i = 1,\dots,r$$

or

Nernst-Planck (NP)

$$J_i = B_i c_i X_i, \qquad i = 1,\dots,r$$

or

Fick (F)

$$J_i = -D_i \ \mathrm{grad}\ c_i, \qquad i = 1,\dots,r$$

Fig. 1. The schema showing the presented method and the available flux formulae's.

Figure 1 shows the schema of the method. The flux can be expressed as pure diffusion, $J_i = J_i^d$ (the formulae F, NP and O), or it can be coupled with the Darken method, $J_i = J_i^d + c_i \upsilon^D$ (DF, DNP and DO). The boundary conditions allow coupling interdiffusion and reactive-diffusion. The following basic methods are available to model the reactive-diffusion:

- the quasi-stationary chemical diffusion of one or more elements in the growing layer, e.g., oxidation, intermetallic phase growth, surface treatment;
- the concentration dependent flux through the interface (e.g., evaporation) or
- arbitrary (postulated or measured) time dependent flux(es) through interface.

2.1. Mass conservation law

We do not consider the chemical and/or other reactions within the diffusion zone and the equation of mass conservation has form:

$$\frac{\partial c_i}{\partial t} + \operatorname{div}\left(c_i \upsilon_i\right) = 0\,, \tag{1}$$

where: $c_i = c_i\left(t,x\right)$ and $\upsilon_i = \upsilon_i\left(t,x\right)$ denote the molar concentration and the velocity of the *i*-th component. Summing up Eqs. (1) for all components, the global conservation law follows:

$$\frac{\partial c}{\partial t} + \operatorname{div}\left(c\upsilon\right) = 0\,. \tag{2}$$

The most general form of the flux used in our method is the Darken-Onsager flux:

$$J_i = \sum_{j=1}^{r} L_{ij} X_j + J_i^D, \qquad i = 1,\dots,r \tag{3}$$

where: J_i and J_i^D denote the overall flux and the Darken flux (drift) of the *i*-th component, respectively, L_{ij} are phenomenological transport coefficients and X_j denotes the force acting on the diffusing component. The Onsager constitutive equations base on the definition of the phenomenological transport coefficients [7]:

$$L_{ii} = c_i B_i \frac{\left(\sum_{k=1, k \neq i}^{r} N_k B_k \right)}{\sum_{k=1}^{r} N_k B_k}, \quad i = j, \quad i = 1, ..., r, \tag{4}$$

$$L_{ij} = -c_i B_i \frac{N_j B_j}{\sum_{k=1}^{r} N_k B_k}, \quad i \neq j, \quad i, j = 1, ..., r, \tag{5}$$

where $N_i = N_i(t, x)$ and $B_i = B_i(N_i, ..., N_r)$ denote molar ratio and mobility.

The transport coefficients in Eq. (5) are symmetrical, i.e., $L_{ij} = L_{ji}, \quad i \neq j$:

$$L_{ij} = -c_i B_i \frac{N_j B_j}{\sum_{k=1}^{r} N_k B_k} = -c_j B_j \frac{N_i B_i}{\sum_{k=1}^{r} N_k B_k} = L_{ji}, \quad i \neq j, \quad i, j = 1, ..., r, \tag{6}$$

The forces in Eq. (3), X_j, are defined as a gradient of the chemical potential:

$$X_j = -\mathrm{grad} \mu_j^{ch} \tag{7}$$

The thermodynamic data in Eq. (7) can be introduced as analytical functions or assuming ideality sweeping statement (a_i = c_i). The mobilities in Eqs. (4)-(5), can depend on concentrations. One should notice that the results and the accuracy of the simulations critically depend on the quality of these descriptions (data).

2.2. Equations of state

The total mass density, $\rho = \rho(t,x)$, the molar concentration, the molar volume, $\Omega = \Omega(t,x)$, and the molar mass, $M = M(t,x)$, are defined by the following standard relations:

$$\rho := \sum_{i=1}^{r} \rho_i = \sum_{i=1}^{r} M_i c_i \,, \tag{8}$$

$$c := \frac{1}{\Omega} = \frac{1}{\sum_{i=1}^{r} N_i \Omega_i} = \frac{\rho}{M} = \frac{\sum_{i=1}^{r} \rho_i}{\sum_{i=1}^{r} M_i N_i} = \sum_{i=1}^{r} c_i \,, \tag{9}$$

where M_i is the molar mass of i-th component and Ω_i denotes its partial molar volume. Total and partial molar volumes obey the following relations:

$$d\Omega(N_1, N_2, ..., N_r) = \sum_{i=1}^{r} \frac{\partial \Omega}{\partial N_i} dN_i = \sum_{i=1}^{r} \Omega_i dN_i \,, \tag{10}$$

$$\Omega(N_1, N_2, ..., N_r) = \sum_{i=1}^{r} \int_{0}^{N_i} \Omega_i dN_i = \sum_{i=1}^{r} \frac{\Omega_i c_i}{c}, \qquad \text{at a moment } t^* \in [0,t], \tag{11}$$

where $\int_0^{N_i} \Omega_i dN_i = \Omega_i N_i$. When molar volumes do not depend on concentration and stresses are negligible, the relation known as Vegard law follows from Eq. (11) [12]:

$$\sum_{i=1}^{r} \frac{\Omega_i}{\Omega} N_i = \sum_{i=1}^{r} \frac{\Omega_i c_i}{\Omega c} = \sum_{i=1}^{r} \Omega_i c_i = 1 \tag{12}$$

In this work we do consider noncompressible processes only. Consequently we assume that partial molar volumes are constant, $\Omega_i = const$. The two different forms of the equation of state can be used:

- the classical Darken postulate of constant molar concentration $c := \sum_{i=1}^{r} c_i = const$ and

- the Vegard law $\Omega(t,x) := \sum_{i=1}^{r} N_i \Omega_i = \frac{1}{c}$, Eq. (12).

2.3 Diffusion flux in multicomponent systems.

The Darken flux, J_i^D, is computed relatively to the volume fixed reference frame:

$$J_i^D = c_i \upsilon^D \tag{13}$$

where: υ^D is Darken velocity that is common for every component.

The Darken velocity, υ^D, is generated during interdiffusion due to locally unbalanced diffusion fluxes [16, 17]. The different partial molar volumes imply:

$$\upsilon^D(t,x) = -\sum_{i=1}^{r} \frac{c_i \Omega_i}{c\Omega} \upsilon_i^d \ . \tag{14}$$

Depending on the available data, the diffusion flux can be expressed by the different constitutive equations. When different partial molar volumes are considered, $\Omega_i \neq \Omega_j,\ i \neq j$ the diffusion fluxes that are defined in the volume fixed reference frame and contain the correction factor, $f_i = \frac{\Omega_i}{\Omega}$ [16]. The following constitutive equations are allowed in the presented method, Figure 1:

a) The Darken-Onsager flux,

$$J_i = \frac{\Omega_i}{\Omega} \sum_{j=1}^{r} L_{ij} X_j + J_i^D, \qquad i = 1,\ldots,r \tag{15}$$

b) The Onsager flux:

$$J_i = \frac{\Omega_i}{\Omega} \sum_{j=1}^{r} L_{ij} X_j, \qquad i = 1,\ldots,r \tag{16}$$

c) The Darken-Nernst-Planck flux[1]:

$$J_i = \frac{\Omega_i}{\Omega} c_i B_i X_i + J_i^D, \qquad i = 1,...,r. \tag{17}$$

d) The Nernst-Planck diffusion flux [18,19]:

$$J_i = \frac{\Omega_i}{\Omega} c_i B_i X_i, \qquad i = 1,...,r \tag{18}$$

e) The Fick-Darken flux[2]:

$$J_i = -D_i \text{ grad } c_i + J_i^D, \qquad i = 1,...,r \tag{19}$$

f) The Fick flux, Eq. (19), without Darken velocity and when molar volumes are equal becomes 1st Fick law:

$$J_i = -D_i \text{ grad } c_i, \qquad i = 1,...,r \tag{20}$$

2.4 Composition dependent diffusivities.

The method allows to introduce constant as well as composition dependent diffusivities for all of the components, e.g., as analytical functions. Other possibility is to approximate the composition dependent diffusivities from the known self diffusion coefficients for each component:

$$D_i^* = D_i^0 \exp\left(-\frac{Q_i}{RT}\right), \qquad i = 1,...r \tag{21}$$

---

[1] Equation (17) follows from (3) when: $L_{ij} = 0$, for $i \neq j$ and $L_{ii} \approx c_i B_i$, $i = 1,...,r$.

[2] Equation (19) follows from Eq. (17). By assuming i) the ideality sweeping statement and ii) the equal partial molar volumes of components and Nernst-Einstein relation between self diffusion coefficient and mobility, $D_i = B_i kT$. One gets: $X_i = -\text{grad}\left(\mu_i^0 + RT \ln c_i\right) = -{}^{RT}\!/_{c_i}\, \text{grad} c_i$, where: μ_i^0 is standard chemical potential, *R* and *T* denote the gas constant and temperature.

where: D_i^0 and Q_i denote the pre-exponential constant and activation energy for diffusion.

Following DICTRA [20], in the spirit of the Calphad approach, the composition dependency of these two factors, is represented with a linear combination of the values at each endpoint of the composition space. Using the Redlich-Kister expansion and Eq. (21) one gets:

$$\Phi^i = RT \ln D_i^* = RT \ln D_i^0 - Q_i, \qquad i = 1,...r \tag{22}$$

where: Φ^i can be interpreted as free energy of diffusion of the *i*-th component.

The intrinsic diffusivities in *r*-component mixture (solid solution) are computed using the following relation [20]:

$$\Phi_i = \sum_{j=1}^{r} N_j \Phi^j + \sum_{j=1}^{r} \sum_{k>j}^{r} N_j N_k \left[\sum_{p=0}^{m} {}^{p}\Phi^{j,k} \left(N_j - N_k \right)^p \right], \qquad i = 1,...r \tag{23}$$

where: Φ_i can be interpreted as free energy of intrinsic diffusion in the alloy, Φ^j is a value of Φ_i for pure *j*-th component and ${}^{p}\Phi^{j,k}$ are binary interaction parameters.

Thus from the Eq. (22), the intrinsic diffusivities in the alloy are given by:

$$D_i = D_i^{alloy} = \exp\left(\frac{\Phi_i}{RT} \right) \qquad i = 1,...r. \tag{24}$$

2.5. Boundary conditions

The diffusion processes can be simulated using different boundary conditions. The software can simulate both the open and closed systems.

1) In closed system all fluxes at all boundaries equal zero,

$$J_i\left(t,0\right) = J_i\left(t, \lambda_R\left(t\right)\right) = 0, \quad i = 1,...r \tag{25}$$

2) The boundary condition in a case of interdiffusion in open systems (system exchanging mass with a surrounding, Fig. 2) states that the flux of the arbitrary element through interface equals its diffusion flux in alloy at interface [10], e.g., for the right boundary it is:

$$J_i^d\left(t,\lambda_R\right)=J_i\left(t,\lambda_R\right), \tag{26}$$

where flux through interface, $J_i\left(t,\lambda_R\right)$, is a known or computed function of time.

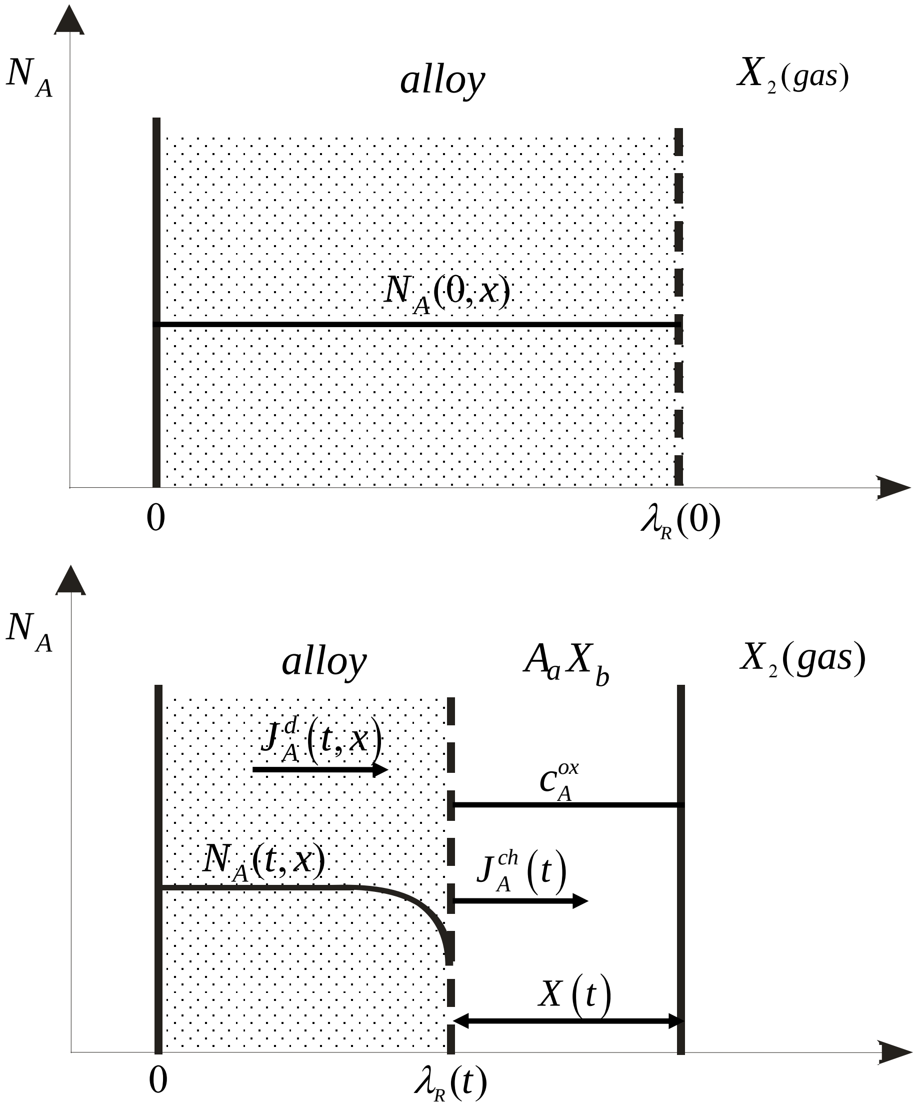

Fig. 2. The schema of the interdiffusion forced by the chemical reaction at alloy|oxide interface.

In this work we consider the fluxes at the boundaries, $J_i\left(t,\lambda_R\left(t\right)\right)$ and $J_i\left(t,0\right)$, that are a result of chemical reaction, $J_i^{ch}\left(t\right)$ [3]:

$$J_i\left(t,\lambda_R\left(t\right)\right)=J_i^{ch}\left(t\right). \tag{27}$$

The reaction flux can be introduced by:

a) the analytical, known function to simulate the arbitrary process, e.g., a surface treatment of the alloy. The user has a possibility to introduce different fluxes for every component.

b) in a case of oxidation the fluxes can be introduced based on the Wagner method [3].

Wagner was first to notice that the oxidized component enters the oxide phase as a result of the surface reaction and of the diffusion through alloy|oxide interface. The non-reacting element diffuse into the interior of the multi-component alloy [3]. By analogy, the reaction flux of A, $J_A^{ch}\left(t\right)$, is due to the surface reaction, $-c_A\left(t,\lambda_R\right)\mathrm{d}\lambda_R/\mathrm{d}t$, and flux of A through the alloy|oxide interface, $J_A\left(t,\lambda_R\right)$, Fig. 2.

$$J_A^{ch}\left(t\right)=-c_A\left(t,\lambda_R\right)\frac{\mathrm{d}\lambda_R}{\mathrm{d}t}+J_A\left(t,\lambda_R\right) \tag{28}$$

The total (volume) balance of A during reaction of the multi-component alloy showing the constant molar concentration requires:

$$J_A^{ch}\left(t\right)=-c\frac{\mathrm{d}\lambda_\mathrm{R}}{\mathrm{d}t} \tag{29}$$

From Eqs. (28) and (29) the flux of A in the alloy at alloy|oxide interface is given by

$$J_A\left(t,\lambda_R\right)=\left(c_A\left(t,\lambda_R\right)-c\left(t,\lambda_R\right)\right)\frac{\mathrm{d}\lambda_R}{\mathrm{d}t}. \tag{30}$$

Above equation is identical with boundary condition in the case of binary Ni-Pt alloy analyzed by Wagner [3]. In a case of multi-component alloy it is necessary to compute inward fluxes of the all non-reacting components. These diffusion fluxes are a result of the alloy consumption: $\mathrm{d}\lambda_R/\mathrm{d}t$. Consequently:

$$J_i\left(t,\lambda_R\right)=c_i\left(t,\lambda_R\right)\frac{\mathrm{d}\lambda_R}{\mathrm{d}t} \quad \text{for} \quad i=1,2,...,r-1 \tag{31}$$

The fluxes in the alloy as given by Eqs. (30) and (31), are computed only when both diffusion and convection are considered, Fig. 1. The schema of the interdiffusion forced by the chemical reaction at alloy|oxide interface is shown in Fig. 2. In a case of low nonstoichiometry of the growing phase, $c_A^{ox} \cong const.$, the flux of the reacting component A depends on time only (does not depend on position) [3]. This flux can be expressed by the Nernst-Planck formula [18,19]

$$J_A^{ch}\left(t\right)=-c_A^{ox}B_A^{ox}\frac{\partial\mu_A^{ox}}{\partial x} \tag{32}$$

The Nernst-Einstein relation, $D_i=B_ikT$ [21], allows writing the reaction flux in the form:

$$J_A^{ch}\left(t\right)=-\frac{c_A^{ox}D_A^{ox}}{RT}\frac{\partial\mu_A^{ox}}{\partial x} \tag{33}$$

The balance of A at the oxide|gas interface (Stefan condition) requires:

$$J_A^{ch}\left(t\right)=c_A^{ox}\frac{\mathrm{dX}}{\mathrm{d}t}. \tag{34}$$

By comparison of the Eqs. (32) and (34), than applying the mean value theorem, one can obtain the rate growth equation, where the reaction rate is a function of time [3]:

$$\frac{\mathrm{d}X}{\mathrm{d}t}=\frac{k\left(t\right)}{X\left(t\right)} \quad \text{where} \quad k\left(t\right)=\frac{1}{RT}\int_{\mu_A''}^{\mu_A'(t)}D_A^{ox}d\mu_A^{ox} \tag{35}$$

where $\mu_A'(t)=\mu_A(\text{alloy}|\text{oxide})$ and $\mu_A''=\mu_A(\text{oxide}|\text{O}_2)$ are the local chemical potentials of A at interfaces, Fig. 2.

Upon assuming the local thermodynamical equilibrium at the alloy|oxide interface,

$$\mu_A(alloy)(t,\lambda(t))=\mu_A(t,\lambda(t))=\mu_A'(oxide)(t), \tag{36}$$

the instantaneous rate constant in Eq. (35) can be expressed as a function of A concentration in the alloy, at the alloy|oxide interface:

$$k(t)=\frac{1}{RT}\int_{\mu_A''}^{\mu_A(t,\lambda_R)} D_A^{ox}\,d\mu_A^{ox} . \tag{37}$$

Equations (34) and (35) allow computing the flux of A in the oxide as a function of the instantaneous rate constant (chemical potential of A at interface):

$$J_A^{ch}(t)=c_A^{ox}\frac{k(t)}{X(t)}=\frac{c_A^{ox}k(t)}{\sqrt{2\int_0^t k(\tau)d\tau}}, \tag{38}$$

where $X(t)^2=2\int_0^t k(\tau)d\tau$.

The interdiffusion in the alloy and the reaction diffusion in the oxide are coupled by the flux of reacting component through the interface, Fig. 2. The total flux of reacting component A, Eq. (38), through the alloy|A$_a$X$_b$ interface is a result of reaction (alloy consumption), Eq. (30). Combining Eqs. (29), (30) and (38), one gets the equation describing the flux of oxidized component through the interface:

$$J_A(t,\lambda_R(t))=\frac{c_A^{ox}k(t)}{\sqrt{2\int_0^t k(\tau)d\tau}} \quad \text{where} \quad k(t)=\frac{1}{RT}\int_{\mu_A''}^{\mu_A(t,\lambda_R)} D_A^{ox}\,d\mu_A^{ox} . \tag{39}$$

2.6. Initial conditions

1) Initial distributions of the mixture components must be known:

$$c_i\left(0,x\right)=c_i^0\left(x\right) \text{ for } i=1,2,...,r \tag{40}$$

The initial distributions of the components can be introduced as a step function (Heaviside function) or any profile given by the set of points. Thus, one can analyze processes in gradient materials, multi-layers, multiples materials and many others.

2) Initial position of the right boundary of the mixture, $\lambda_R\left(0\right)=\lambda_R^0$ (the thickness of the mixture/alloy).

3) Initial thickness of the product layer, $X\left(0\right)=X^0$

3. Examples

3.1. The reaction-diffusion, processes at different time scales

From the technical point of view, very interesting are the heterogeneous reactions, e.g., the oxidation of alloys, some CVD processes, etc. In such processes three different phases are considered. Figure 2 shows the substrate (the multi-component alloy), reacting element in gas or liquid phase (oxidant X) and solid product layer (A_aX_b). The respective interfaces are planar and local equilibrium is assumed.

Reaction-diffusion, non stationary Wagner model. Heterogeneous reactions in many cases result in the formation of the compound showing narrow homogeneity range, i.e., showing the low nonstoichiometry, $A_{a-y}X_b$, where $y\approx 0$. In this work we analyse growth of the binary compound shown on Fig. 2. The A-component of the alloy reacts with, X-component in the gas atmosphere, X_2(gas). The slowest, rate controlling process is diffusion of A and/or X in the growing product layer of finite thickness, $X(t)$, Fig. 2. The compound formation occurs according to reaction:

$$a\mathrm{A(alloy)} + {}^{b}\!/_{2}\mathrm{X}_2(\mathrm{gas}) = \mathrm{A}_a\mathrm{X}_b . \tag{41}$$

Let us assume that the alloy is an ideal solid solution, $\mu_i = \mu_i^0 + RT\ln c_i$. The local equilibrium at $\lambda_R(t)$, Eq. (36), implies $\mu_A'(oxide)(t) = \mu_A^0 + RT\ln c_A(t,\lambda(t))$. In such a case the instantaneous rate constant in Eq. (39) becomes:

$$k(t) = \int_{c_A''}^{c_A'(t)} D_A^{ox} d\ln c_A \tag{42}$$

or

$$k(t) = \int_{N_A''}^{N_A'(t)} D_A^{ox} d\ln N_A \tag{43}$$

where: $N_A'(t) = N_A(t,\lambda_R(t))$ is a molar ratio of the component A in the alloy at the alloy|oxide interface.

Following Wagner, the molar ratio of the oxidized component A in the oxide can be expressed assuming the local equilibrium within the scale. Consequently, the oxidized component mole fraction at the alloy|oxide interface is given by [3]:

$$\left(N_A'(t)\right)^{4/z} p_{O_2}'(t) = p_{O_2}'^{(e)} \tag{44}$$

where: $p_{O_2}'(t)$ and $p_{O_2}'^{(e)}$ denote the oxygen partial pressures at the alloy|oxide and (pure metal A)|oxide interfaces respectively, z is the valence of oxidized component A in oxide. Combining Eqs. (43) and (44):

$$k(t) = \frac{z}{4}\int_{p_{O_2}'(t)}^{p_{O_2}''} D_A^{ox} d\ln p_{O_2} \tag{45}$$

where $p_{O_2}'(t) = p_{O_2}(\mathrm{alloy}|\mathrm{oxide})$ and $p_{O_2}'' = p_{O_2}(\mathrm{oxide}|\mathrm{O}_2)$ are the oxygen pressures at interfaces of the growing layer.

It was shown by authors, that presented method gives better approximation of the experimental data than the Wagner quasi-stationary solution [22].

Reaction-diffusion, arbitrary ternary alloy. In this work we show the influence of the different time scales, different diffusion coefficients in alloy and oxide.

The data used to simulate the oxidation of the arbitrary ternary alloy are shown in Table 1. We assume that it is an ideal solid-solutions and that intrinsic diffusivities in an alloy and oxide differ (interdiffusion coefficient in alloy depends on composition).

Table 1. Data used to simulate the oxidation of the A-B-C alloy: $N_A(0)$=0.6, $N_B(0)$=0.1, $N_C(0)$=0.3 and the initial thickness of oxidized alloy equals 50 µm.

	$D_A^{ox(0)}\left[\frac{cm^2}{s}\right]$	$D_i\left[\frac{cm^2}{s}\right]$	$c_A^{ox}\left[\frac{mol}{cm^3}\right]$	$p'^{(e)}_{O_2}\ [atm]$	$p''_{O_2}\ [atm]$	$k_C^0\left[\frac{cm^2}{s}\right]$
a)	$5.0\cdot10^{-15}$	$D_A=1.0\cdot10^{-13}$ $D_B=1.0\cdot10^{-14}$ $D_C=5.0\cdot10^{-15}$	$8.0\cdot10^{-2}$	$1.0\cdot10^{-20}$	0.21	$1.16\cdot10^{-14}$
b)	$5.0\cdot10^{-15}$	$D_A=1.0\cdot10^{-15}$ $D_B=1.0\cdot10^{-14}$ $D_C=5.0\cdot10^{-13}$	$8.0\cdot10^{-2}$	$1.0\cdot10^{-20}$	0.21	$1.16\cdot10^{-14}$

Figure 3 shows the results obtained for an arbitrary ternary alloy, A-B-C. It can be seen that when intrinsic diffusivities in the alloy are higher than in the growing layer, Fig. 3a, then the oxidation process can be approximated by the parabolic rate law, i.e., the slow diffusion in the reaction product is rate controlling step. One may also note relatively high concentration of reacting element A in the alloy at the alloy$\,|\,$oxide interface. The low intrinsic diffusivities in the alloy markedly decrease the reaction rate, Fig. 3b. The concentration of reacting metal in alloy at alloy|oxide interface after the long reaction time decreases to the very low values and oxidation process is non-parabolic one.

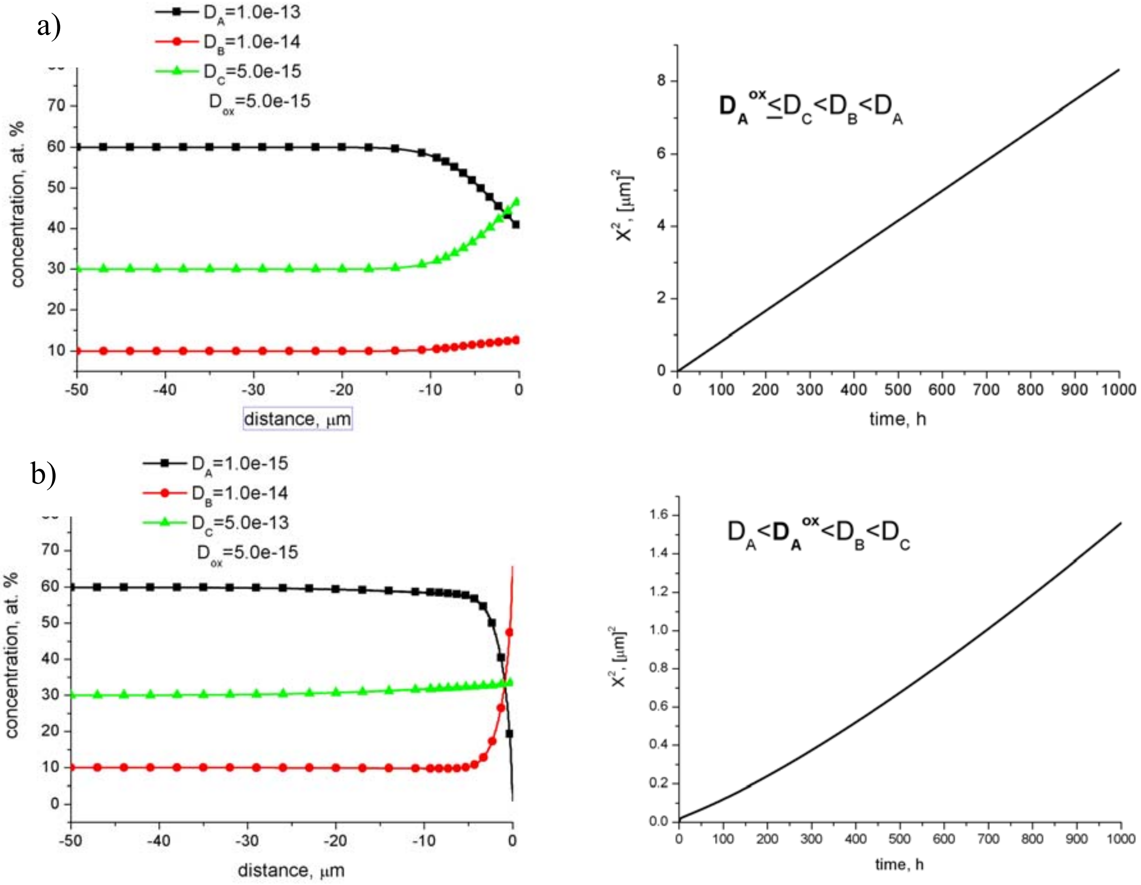

Fig. 3. The growth rate of the AO scale on ternary alloy and concentrations of components as a function of distance from alloy/oxide interface after 1000 hours.

The last example is the reactive-interdiffusion is again selective oxidation of the arbitrary ternary gradient material (alloy). The initial concentration of components shown in Fig. 4 is typical for the alloy | coating system. The data used to simulate the interdiffusion and reaction of the arbitrary ternary alloy are shown in Table 2.

Table 2. Transport properties of the ternary alloy and oxide, AX.

$D_A^{ox(0)}\left[\frac{cm^2}{s}\right]$	$D_i\left[\frac{cm^2}{s}\right]$	$c_A^{ox}\left[\frac{mol}{cm^3}\right]$	$p'^{(e)}_{O_2}\ [atm]$	$p''_{O_2}\ [atm]$	$k_C^0\left[\frac{cm^2}{s}\right]$
$5.0\cdot10^{-15}$	$D_A=1.0\cdot10^{-13}$ $D_B=1.0\cdot10^{-14}$ $D_C=5.0\cdot10^{-13}$	$8.0\cdot10^{-2}$	$1.0\cdot10^{-20}$	0.21	$1.16\cdot10^{-14}$

The initial thickness of the alloy equals 100 µm, oxidation time equals 10000 h.

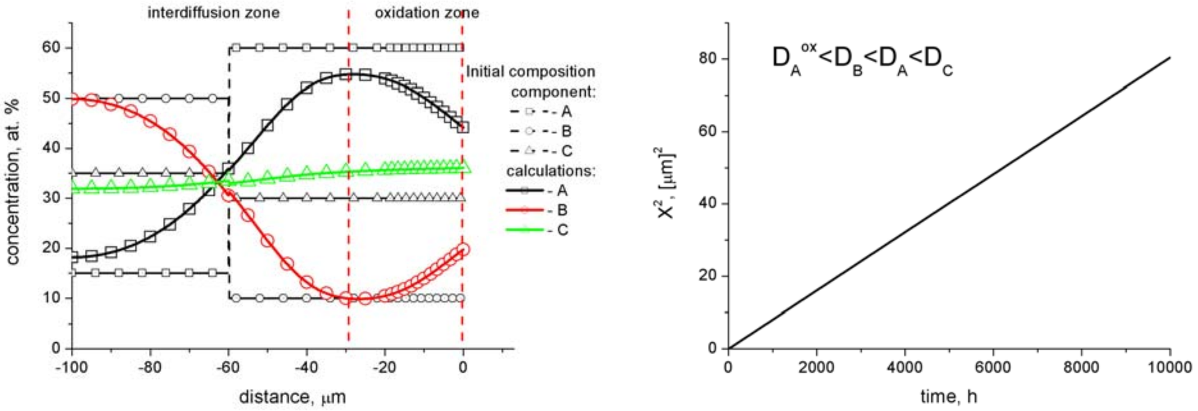

Fig. 4. The thickness of the AO scale growing on A-B-C ternary alloy/coating system after 10000 hours; the concentration of components as a function of distance from the coating/oxide interface.

It can be seen that live time of the material exceeds 10000 hours and process follows the parabolic rate law.

3.2. Interdiffusion

In this section we compare the experimental results [23] with the computed results using the Darken-Nernst-Planck flux formulae, Eq. (17). The Fe-Cu-Ni system was chosen because it is a single phase in a wide range of compositions and the extensive experimental data are available. The following data were used:

- the thermodynamic properties of Fe-Cu-Ni alloys at $T = 1273$ [K] [24];
- the experimentally measured tracer diffusivities in Cu-Fe-Ni alloys [25];
- the composition of diffusion couple: 41.9NCu-58.1Ni|Fe [wt.%], its thickness: 2 [mm] ± 0.1 and annealing time: 170 [h] [23];
- the partial molar volumes of components, Ω_i, were estimated from the density of the pure metals and relation: $\Omega_i = M_i / \rho_i^T$. The density of alloy, ρ^T, was estimated using the expression: $\rho^T = \rho^{T_m} - k\left(T - T_m\right)$ where T_m is an alloy melting temperature, ρ^{T_m} its density and k the coefficient of thermal expansion [26]. The partial molar volumes equal: $\Omega_{Cu} = 7.92$, $\Omega_{Fe} = 7.66$, $\Omega_{Ni} = 7.21$ [cm^{3}mol^{-1}].

Figure 5 shows the comparison of the experimental data [23] with computed results. Figure 6 shows the results obtained with the use the composition dependent diffusivities (section 2.4) and the average intrinsic diffusion coefficients: $D_{Cu} = 1.021 \cdot 10^{-9}$, $D_{Fe} = 1.254 \cdot 10^{-10}$ and $D_{Ni} = 3.647 \cdot 10^{-12}$ $\left[cm^2/s\right]$ [25].

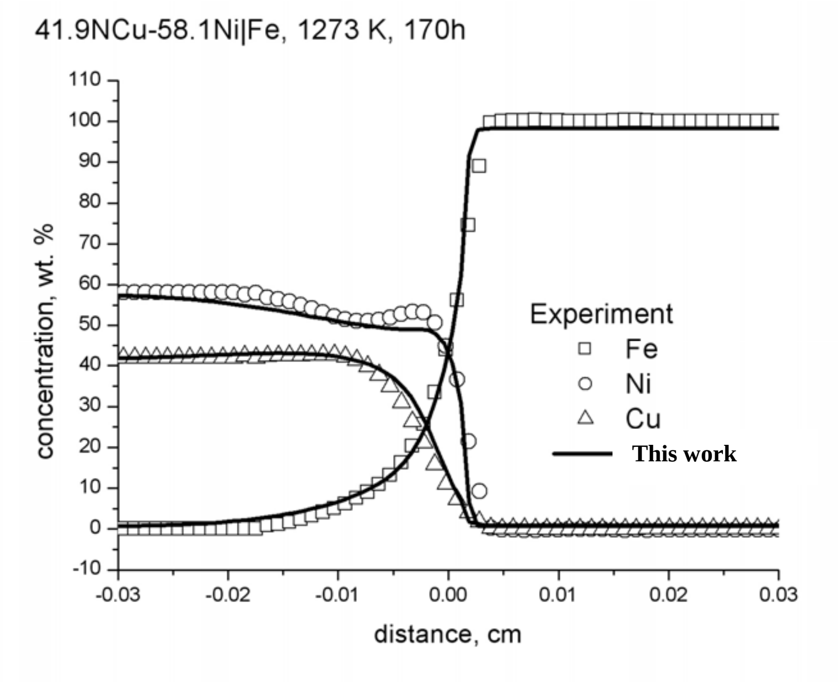

Fig. 5. Comparison of the experimental and calculated distribution of elements in the 41.9NCu-58.1Ni|Fe [wt.%] diffusion couple.

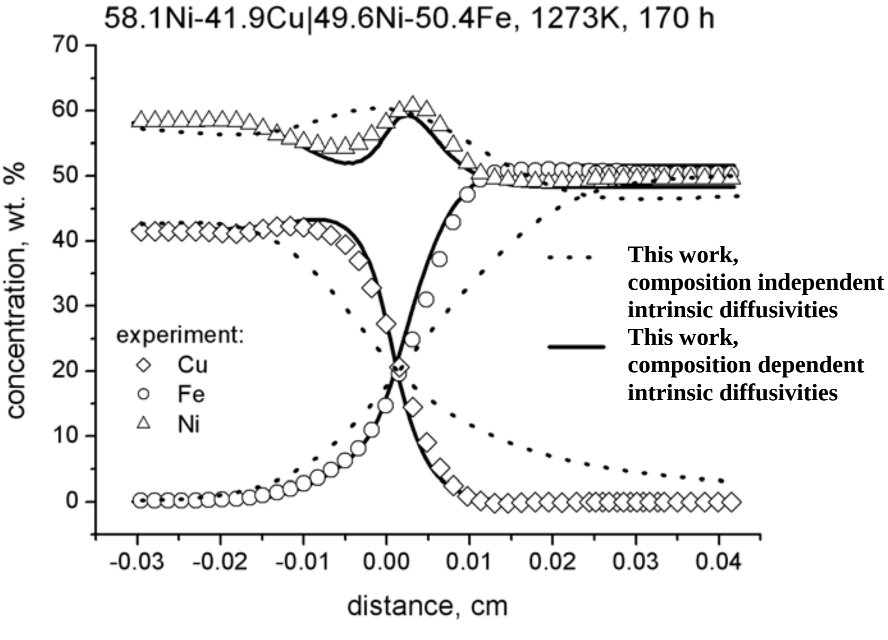

Fig. 6. The comparison of different approximation of diffusion coefficient

It is evident that the approximation give satisfactory agreement with experimental results in case of simulating the Cu-Fe-Ni diffusion couple 58.1Ni-41.9NCu|49.6Ni - 50.4Fe [wt. %] [23].

4. Summary and conclusions

We presented the model of the reaction–diffusion in the multi-component, two-phase system. The simulation of interdiffusion in ternary alloy and the selective oxidation of the binary/ternary compound validated model. The simulation of interdiffusion in the Fe-Ni-Cu alloy show satisfactory agreement with experimental data. Moreover, it confirms the effectiveness of the approximation method used to evaluate the intrinsic diffusivities as a function of concentration.

The model/method and the software can be extended to compute the more complex processes.

Acknowledgement

The authors wish to thanks Dr R. Filipek for providing thermodynamical data. This work has been supported by the Ministry of Science and Higher Education of Poland project **COST/247/2006**.

References.

---

[1] C. Wagner, J. Electrochem. Soc. 103 (1956) 571

[2] C. Wagner, J. Electrochem. Soc. 103 (1956) 627

[3] C. Wagner, J. Electrochem. Soc. 99 (1952) 369

[4] C. Wagner, Z. Elektrochem. 63 (1959) 772

[5] V. I. Dybkov, Reaction Diffusion and Solid State Chemical Kinetics, The IPMS Publications, Kyiv 2002.

[6] H. Schmalzried: „Chemical Kinetics of Solids”, John Wiley and Sons Ltd, 1995.

[7] G.E. Murch and I. V. Belova, Phenomenological Coefficients n Solid-State Diffusion: an Introduction, Diffusion fundamentals 2, 2005, 8.1-8.13

[8] J.R. Manning, Z. Naturforsch. **26a**, 1971, 69

[9] L.S. Darken, Trans. AIME, 174 (1948) 184

[10] K. Holly, M. Danielewski , Physical Reviev B, 50 (1994) 13336

[11] M. Danielewski, R. Filipek, Journal of Computational Chemistry 17 (1996) 1497

[12] L. Vegard, Z. Phys. **5** (1921) 17

[13] V. Kouznetsova, M. G. D. Geers and W. A. M. Brekelmans, Int. J. Numer. Meth. Eng. 54 (2002) 1235–1260.

[14] T. I. Zohdi and P. Wriggers, Introduction to Computational Micromechanics, Springer, 2005.

[15] M. Danielewski and M. Wakihara, “Kinetic Constraints in Diffusion”, Defect and Diffusion Forum, 237-240, 151 (2005).

[16] Danielewski M., Wierzba B.: “Mechano-Chemistry; Diffusion in Multicomponent Compressible Mixtures”, Physica A 387 (2008) 745,

[17] B. Wierzba, M. Danielewski, R. Bachorczyk-Nagy, M. Pietrzyk, Defect and Diffusion Forum **264** (2007) 47

[18] W. Nernst, Z. Phys. Chem. 4 (1889) 129

[19] M. Planck, Ann. Phys. Chem. 40 (1890) 561

[20] Dictra User’s Guide, Version 21., www.thermocalc.com/Products/Dictra.html

[21] A. Einstein, Annalen der Physik **17** (1905) 549

[22] M. Danielewski, B. Wierzba, Diffusion Processes Determining the Oxidation Rate of Multicomponent Alloys, Corrosion Science (2007), doi: 10.1016/j.corsci.2007.11.024

[23] R. Bachorczyk-Nagy: “Metody wyznaczania współczynników dyfuzji i ewolucja składu w stopach wieloskładnikowych”, PhD thesis, Kraków 2002 (in polish).

[24] Rönkä K. J., Kodentsov A. A., Loon P. J. J., Kivilahti J. K., Loo F. J. J.: “Thermodynamic and Kinetic Study of Diffusion Paths in the System Cu-Fe-Ni”, Metall. Trans. A, **27A**, 1996, s. 2229

[25] S.V. Divinski, F. Hisker, C. Herzig, R. Filipek and M. Danielewski: ”Self- and Interdiffusion in Ternary Cu-Fe-Ni Alloys”, Defect and Diffusion Forum, 2005, **237-240**, pp. 50-61.

[26] D.R. Lide, CRC Handbook of Chemistry and Physics, 79th Edition, 1998-1999.